Electrogenerated chemiluminescence at droplet-modified electrodes: towards biphasic pK_a measurement *via* proton-coupled electron transfer at liquid|liquid interfaces

Carlos Lledo-Fernandéz,[a] Imren Hatay,[ab] Michael J. Ball,[a] Gillian M. Greenway[a] and Jay Wadhawan*[a]

Received (in Montpellier, France) 26th June 2008, Accepted 17th October 2008
First published as an Advance Article on the web 5th January 2009
DOI: 10.1039/b810844g

This preliminary work reports, for the first time, electrogenerated chemiluminescence (ECL) at droplet-modified electrodes. The system involves oxidation of aqueous tris(2,2′-bipyridyl)ruthenium(II) ions at a glassy carbon electrode on which a random array of microdroplets of a highly hydrophobic tertiary amine (trioctylamine) are immobilised. Luminescence, produced *via* electron transfer over the cupola surface of the droplets from the oil to aqueous tris(2,2′-bipyridyl)ruthenium(III) ions synthesised *via intra muros* electrochemical oxidation at the uncovered parts of the electrode surface, is demonstrated. The extent of ECL production is shown to be dependent on the degree of interfacial protonation, with a proton-coupled biphasic electron transfer reaction occurring when the liquid|liquid interface is fully protonated, changing to a biphasic outer-sphere electron transfer mechanism when the interface is fully deprotonated. The competition and gradual dominance of one of these extreme mechanisms under intermediate interfacial protonation conditions thence enables the sensitive, kinetic estimation of the biphasic pK_a.

1. Introduction

The proton-transfer reaction is the most uniquely simple and fascinating form of positive charge transfer in chemistry, stemming from the fact that such processes occur *via* the movement of a nucleus stripped of any surrounding electrons.[1] In biology, acid–base regulation is fundamentally important.[2] From a technological perspective, the performance of current state-of-the-art biofuel cells, which employ dehydrogenases[3] crucially depend on proton-transfer events. Although on a macroscopic level proton-transfer within homogeneous solution may be considered as a first approximation in deducing the physico-chemical factors governing the pH dependence of enzyme reactions, this approach is not valid when probing the dynamics of proton transfer (*viz.* pK_a and state of ionisation) in restricted media such as that in the vicinity of the localised sites of the functional groups involved in enzymic catalysis to a microscopic detail. In this case, the folded, glutinous protein architecture exhibited by enzymes creates a confined environment for proton transfer, affecting the acid/base properties of water molecules by virtue of disrupting its hydrogen-bonded structure,[4,5] so that Brønsted acidity is better described in terms of "proton transfer efficiency", parameterised by the rate constants for deprotonation (k_f) and protonation (k_b) of the substrate (A or AH^+, *q.v.* eqn (1)), rather than by the classical notion of pH:

$$AH^+ \underset{k_b}{\overset{k_f}{\rightleftharpoons}} A + H^+ \qquad (1)$$

Note that in the above equation, it is improper to provide the proton with its usual aqueous state symbol, since its micro-confined bathing medium is in an altered state *cf.* bulk water. If the protonated and deprotonated states, referred to as AH^+ and A respectively, are freely diffusible entities, of activity a_i (i = AH^+ or A), we may write the corresponding dissociation constant, K_a:

$$K_a = \frac{k_f}{k_b} = \frac{a_A a_{H^+}}{a_{AH^+}} = \frac{\gamma_A \gamma_{H^+}}{\gamma_{AH^+}} \frac{c_A c_{H^+}}{c_{AH^+}} \qquad (2a)$$

where γ_i and c_i, respectively refer to the activity coefficient and bulk concentration of species i. It follows that heterogeneous protonation kinetics furnish an heterogeneous dissociation constant, hereafter described by the term $K_a^{biphasic}$:

$$K_a^{biphasic} = \frac{k_f}{k_b} = \frac{\Gamma_A}{\Gamma_{AH^+}} a_{H^+}^{surf} = \frac{\Gamma_A^2}{\Gamma_{AH^+}} f_{H^+} = \frac{\Theta_A \Gamma_A}{\Theta_{AH^+}} f_{H^+} \qquad (2b)$$

in which Γ_i refers to the surface concentration of species i, Θ_i is the normalised surface concentration of species i, and we recognise that the activity of the expelled surface protons ($a_{H^+}^{surf}$) is directly proportional to the amount of the deprotonated form (A) of the surface-localised species (assuming it to be monobasic), for which the activity coefficient (f_{H^+}) is tantamount to an adsorption coefficient reflecting the

[a] *Department of Physical Sciences (CHEMISTRY), The University of Hull, Cottingham Road, Kingston-upon-Hull, UK HU6 7RX*
[b] *Department of Chemistry, Selçuk University of Konya, Campus 42075 Konya, Turkey. E-mail: j.wadhawan@hull.ac.uk. URL: http://www.hull.ac.uk/chemistry/wadhawan; Fax: +44 (0) 1482 466 416; Tel: +44 (0) 1482 466 354*

binding of the protons to the basic surface, and the degree of non-ideality both in solution and on the surface.†

It follows from eqn (2b) that, should we have a technique for measuring the relative amounts of AH^+ and A at the soft matter|water interface, the calculation of $K_a^{biphasic}$ is possible (on making assumptions about the proton activity coefficient). Accordingly, under the assumption that molecular-scale local environment perturbations can be neglected, much work has been undertaken using molecular chemical probes, specifically fluorescent acid–base indicators to extract the rate constants for deprotonation and back-recombination from time-resolved spectral measurements.[4,5,8] Such exquisite experiments provide information on the location of the chemical fluorophore and the corresponding ability of the microenvironment to accept protons,[8] and indicate, as anticipated above, that efficiency and proton-transfer kinetics are strongly location-dependent; the smaller the size of the confined microenvironment, the longer is the fluorescent decay, owing to the greater probability of recapturing photochemically-induced proton ejection *via* geminate recombination.[4]

Given the powerful and exquisite sensitivity of light in providing data on micro-chemical architecture, we sought to use visible luminescence produced electrochemically in aqueous solution to explore the visualisation of the molecular design of an electrode surface coated with an array of femtolitre oil microdroplets randomly sprinkled over the electrode surface.‡ This is a non-traditional liquid|liquid system, recently pioneered by several research groups.[21,22] These systems represent an excellent biomimetic methodology since they actually reflect a picture more accurately of the structure of biological membranes that make up, *inter alia*, cell boundaries; by immobilising an oil at random on a solid electrode surface (with fractal dimension of between two and three), and immersing this into an aqueous electrolyte, in which the oil phase is insoluble, enables the creation of a series of oil|water interfaces that are separated by solid|water interfaces, the latter arising from the parts of the electrode that are not modified, and the whole description of the microchemical interface accounts for the dispersion of active sites within biological membranes. It is noteworthy that in this scenario, provided that the interdroplet spacing is and elegantly explored this technique for the spatially-resolved imaging of the diffusion layer of ensembles of electrodes of micrometric and sub-micrometric dimensions. In brief, when a strong electron donor (D^-) reacts, *via* homogeneous electron exchange, with a strong electron acceptor (A^+), either of which, or both, may have been electrochemically synthesised, the Gibbs energy of this highly exothermic reaction is greater than the reorganisation energy; the intersection of the ground-state free energy parabolas of the reactants and products yields a large energy barrier compared with the intersection of ground-state parabola of the reactants with that for the products in which one product is in an excited state.[9] Accordingly, a fraction $(1 - \delta)$ of the electron transfer reaction proceeds non-adiabatically *via* the Marcus inverted region to furnish the reduced form of the electron acceptor in a ground state, whilst the remaining fraction (δ) undergoes electron transfer to a more accessible electronically excited product state (A* or D*) *via* the normal region, since the rate at which the excited state is generated is kinetically faster than the formation rate of ground state products. This excited state can deactivate *via* photon emission (ECL), or alternatively, in the case of the formation of ground state products in high vibronic levels, *via* thermal relaxation (see eqn (F1a)). In homogeneous solution, eqn (F1a) is kinetically rapid and occurs with a bimolecular rate constant close to the Smoluchowski diffusion limit (*ca.* 10^9–10^{10} M^{-1} s^{-1}),[13] since D^- and A^+ instantaneously annihilate each other; they cannot co-exist. This is not necessarily the case in an anisotropic medium, such as that afforded by a liquid|liquid interface, where the reactants can be physically separated *via* location in different phases. However, the groups of Bard[14] and Unwin[15] have been able to demonstrate ECL or inverted electron transfer at liquid|liquid interfaces, primarily using a "top-down" approach, scanning electrochemical microscopy, SECM. The rate of interfacial outer-sphere electron transfer for the case of a liquid|liquid system has been studied theoretically by Marcus,[16] following preliminary studies by Geblewicz and Schiffrin.[17] Two cases have been noted: for a "sharp" liquid|liquid interface, the second-order rate constant, k_{12} is described by eqn (F2a); in contrast, for a "diffuse" interface which encompasses a boundary thickened by the mixing of the solvents, eqn (F2b) is appropriate. Recent works by Schlossman[18a,b] and Richmond[18c] on interfacial structure suggest the latter model is not really fully acceptable.

$$D^- + A^+ \rightarrow D + (1 - \delta)A + \delta A^* \quad (\text{or, } A + (1 - \delta)D + \delta D^*) \qquad \text{(F1a)}$$

$$A^* \rightarrow A + h\nu \ (\text{or, } D^* \rightarrow D + h\nu) \qquad \text{(F1b)}$$

In those equations, which are not directly applicable to biphasic proton-coupled electron transfer in Eigen acids[1] as they have not been derived from coupled proton and electron co-ordinates and therefore cannot account for proton tunnelling through the activation barrier,[19] a_1 and a_2 represent the radii of the reactants (ascribed by the suffixes 1 and 2), separated by a distance x (Δx is the tunnelling decay parameter generally referred to using the symbol β),[16d] ν_n is a typical frequency of molecular motion and κ is a nonadiabatic factor at the distance of closest approach (typically $\kappa\nu_n = 10^{12}$ s^{-1}),[16] F is the Faraday constant, R is the molar gas constant, T is the absolute temperature, $\Delta G^{\ddagger}$ is the change in Gibbs energy for reaction activation, and L is the thickness of the interfacial mixed-solvent layer. Eqn (F2) indicates that it may be possible, from biphasic reaction kinetics measurements, to discern interfacial structure. Indeed, such measurements, elegantly undertaken by Kanoufi *et al.*[14b] for a benzonitrile|water system suggests that ECL occurs *via* electron transfer over an interface 2 nm thick. Accordingly, the kinetics measured ($k_{12} = 0.054$ M^{-1} s^{-1}) for their biphasic system of oxalate oxidation by electrochemically generated $Ru(bpy)_3^{3+}$ is seven orders of magnitude smaller than in homogeneous solution (7×10^5 M^{-1} s^{-1}),[14b] testifying to the fact that the introduction of physical anisotropy can stabilise the co-existence of strong electron donors with strong electron acceptors. Nevertheless, that the kinetics are finite, allows a degree of reactant annihilation of the type indicated in eqn (F1a). It should be noted that quasi-biphasic environments, such as that offered by electrodes supporting self-assembled monolayers still permit very fast ECL kinetics.[20]

$$k_{12} = 2\pi(a_1 + a_2)(\Delta x)^3\kappa\nu_n\exp(-F\Delta G^{\ddagger}/RT) \qquad \text{(F2a)}$$

$$k_{12} = 4\pi(a_1 + a_2)^2(\Delta x)L\kappa\nu_n\exp(-F\Delta G^{\ddagger}/RT) \qquad \text{(F2b)}$$

† Alternatively, we note that at the protonated interface, the electrostatic potential (φ) needs to satisfy Poisson's equation, $\text{grad}(\varepsilon)\text{grad}(\varphi) + \varepsilon\text{div}[\text{grad}(\varphi)] = -F\sum_i z_i c_i$, where ε is the permittivity, F is Faraday's constant, z_i and c_i are the charge and concentration of species i. This simplifies on considering only the aqueous part: $\text{grad}(\varepsilon) = 0$ for a homogeneous linear dielectric.[6] In this case, as the ions in the diffuse region of the resulting electrical double layer are in equilibrium, the gradient of the electrochemical potential therefore vanishes, and the activity of the protons on the surface is given *via* a Boltzmann distribution in the electrostatic surface potential, χ: $a_{H^+}^{surf} = a_{H^+}^{bulk}\exp(-q_0\chi/k_BT)$, where q_0 is the electron charge, and k_BT represents the thermal energy of the system.[7] Note that, strictly, χ is the potential, the gradient of which is equivalent to the average force acting on an ion (the potential of mean force), whereas φ is the canonical ensemble average of the electrostatic potential (the local average potential). The differences between these can be neglected.[7]

‡ Electrogenerated chemiluminescence, ECL,[9] is an incredibly powerful tool for surface structure resolution when viewed in conjunction with a microscope; following the work by Engström at microelectrodes,[10] Amatore and co-workers,[11] and Sojic *et al.*[12] have recently

molecularly-thin (this is possible with high droplet coverages[23]), the interdroplet environment is actually transformed to the restricted aqueous medium described earlier. In most of the previous work,[21,22] the oil phase is redox active, enabling electron transfer to take place between the electrode and the electrochemically unsupported oil microdroplet. Such processes are thought to occur at the base circumference of each individual microdroplet, the locus of which is a three-phase boundary since the oil exists in the presence of both the electrode support and the aqueous electrolyte into which the droplet-modified electrode ensemble is immersed.[24] Material transport within the restricted ambiance of the oil phase is thought to take place *via* migration–diffusion coupled with a degree of Marangoni convection,[25] most likely emanating from microscale phase separation *via* ionic liquid formation upon charge transfer between the electrode and the oil phase due to counter ion insertion from the aqueous phase as a result of electroneutrality conservation within the former phase.[26]

Such droplet-modified electrodes are ideal at which to study ECL phenomena—a single surface plays a dual rôle as "generator"—reactive species may be electrochemically synthesised in controllable amounts at the unexposed parts of the electrically conducting surface, whilst allowing aqueous|oil biphasic reactions to occur over the spherical cap surface of the femtolitre-sized oil deposit, thence allowing the electrode to "collect" informations regarding the extent of the liquid|liquid reaction.§ This paper seeks to address the question as to whether such liquid|liquid electron transfer processes can occur, as observed *via* light synthesis, and whether the quantity of light produced enables extraction of the degree of interfacial protonation. Our system consists of a random array of microdroplets of trioctylamine (Oc_3N) covering the surface of a glassy carbon electrode, which is bathed by an aqueous solution containing tris(2,2′-bipyridyl)ruthenium(II). The trioctylamine is immeasurably insoluble in water, and likewise, the $Ru(bpy)_3^{2+/3+}$ complexes are only soluble in the aqueous phase. Electrogeneration of $Ru(bpy)_3^{3+}$, *via* oxidation at the naked parts of the glassy carbon electrode, enables electron transfer to take place over the surface of the Oc_3N deposits (the liquid|liquid interface): the reducing agent is Oc_3N (or $Oc_3N^{\bullet}$), and the electron is transferred to the π* orbital of one of the bipyridine ligands.[9b,28] ECL is then produced *via* the decay of the excited $Ru(bpy)_3^{2+*}$ state to the ground electronic configuration. The ECL response is significantly affected by the pH of the surrounding aqueous medium, suggesting the observation of light can be correlated to the degree of interfacial protonation, allowing for a kinetics-based measurement of surfacial pK_a.

2. Experimental

Chemical reagents

All chemical reagents used to prepare aqueous electrolyte solutions were purchased in their purest commercially available forms from Aldrich. HPLC grade dichloromethane (for the deposition procedure) was purchased from Fisher Scientific, Ltd. and used without further purification. All aqueous solutions were made up with water (of resistivity of not less than 18 MΩ cm) taken from an Elgastat filter system (Vivendi, Bucks., UK). These aqueous solutions were saturated with trioctylamine, so as to ensure dissolution kinetics were not measured, and were degassed with oxygen-free nitrogen (BOC Gases, Guildford, Surrey, UK) prior to experimentation; all experiments were undertaken at 23 ± 2 °C.

Instrumentation

Electrochemical experiments were conducted in a conventional three-electrode borosilicate glass cell with a flat bottom, using a 3.0 mm diameter glassy carbon working electrode (Bioanalytical Systems, Inc., UK), a nickel wire counter electrode, and a saturated calomel electrode (SCE, Radiometer, Copenhagen, Denmark). As this electrode can be sensitive to high concentrations of perchlorate anions (due to the precipitation of insoluble potassium perchlorate at the calomel frit), this electrode was replaced in some experiments with a sodium-saturated calomel electrode (SSCE). All results reported in this paper are, however, corrected to the SCE. Electrochemical data were recorded using a commercially available computer-controlled potentiostat (Autolab PGSTAT30, Eco Chemie, Utrecht, Netherlands, or PalmSens Instruments device). The glassy carbon working electrode was modified with trioctylamine microdroplets by solvent evaporation of an aliquot of *ca.* 1 mM redox oil dichloromethane solution. Before being immersed, this droplet-modified electrode was inverted and held over the degassing aqueous phase for at least ten minutes (so as to remove oxygen from the oil phase).¶ The electrode was cleaned by rinsing with dichloromethane and polishing on a napped polishing cloth using 0.3 μm alumina slurry (Presi, France) immediately prior to experimentation.

For electrochemiluminescence experiments, the electrochemical cell was positioned on top of a miniaturised photomultiplier tube with maximal sensitivity close to the 610 nm photon produced in this work[29] (H5784-20, Hamamatsu Photonics, Enfield, UK, borosilicate window, range $300 \leq \lambda/\text{nm} \leq 920$, peak wavelength of 630 nm) protected by a shutter. The latter was opened for data recording after the whole apparatus had been placed in the dark, so as to minimise the background

§ Compared with the "top-down" approach of SECM, this droplet-modified electrode approach enables competition between diffusional loss and biphasic reaction over a curved surface. The added advantage of such an electrode architecture is that in the vicinity of the oil deposit, material transport to an otherwise unblocked, planar surface transforms into a non-linear diffusion regime.[23,27] Work pioneered first by Amatore and Savéant,[27] and subsequently by Compton *et al.*,[23a,b] has demonstrated that this effect is tantamount to modifying the Butler–Volmer heterogeneous rate constant for electron transfer kinetics at the uncovered parts of the electrode surface (k_s) to $k_s(1-\theta)$, where θ represents the fraction of the conductive surface that is blocked. Recently, Compton and Davies[23c–f] have extended this work to deduce, *via* numerical simulation, the three-dimensional particle size and geometry of the blocking deposit,[23e] and the electrocatalytic reaction kinetics over the surface of such droplet deposits,[23c–f] which suggests that droplet exhaustion *via* electron transfer reaction and solvent polarity effects are significant protagonists in understanding the mechanistic reaction kinetics.

¶ It was observed that oxygen did not have a significant influence on the experimental data. Note that no attempt was made to quantify the amount of ambient dust particles at the liquid|liquid interface; whilst this may play an important rôle, it was neglected herein.

recording of daylight. The chemiluminescence signal was recorded using a chart recorder (Chessel Ltd., Worthing, Sussex); ECL experiments were only undertaken when the background signal had stabilised. The ECL data were not subjected to any *post factum* correction for the absorbance of the borosilicate glass, nor for the distance between the electrode in solution and the bottom of the cell; small changes in the latter had little effect on the data reported herein.

3. Results and discussion

Below, we first consider the voltammetry of the individual components of the biphasic system; we next consider the electrochemistry when both oil and chemical oxidant are present in the investigated system.

3.1 Voltammetry of Oc_3N microdroplets

Fig. 1(a) illustrates the voltammetry of a glassy carbon electrode coated with microdroplets of trioctylamine at a scan rate of 0.1 V s^{-1} immersed into phosphate buffer solution containing 0.1 M sodium perchlorate at a variety of pH values. Previous work in both experiments and modelling[23,30] suggests that, for the amount of Oc_3N employed herein, droplet radii are typically

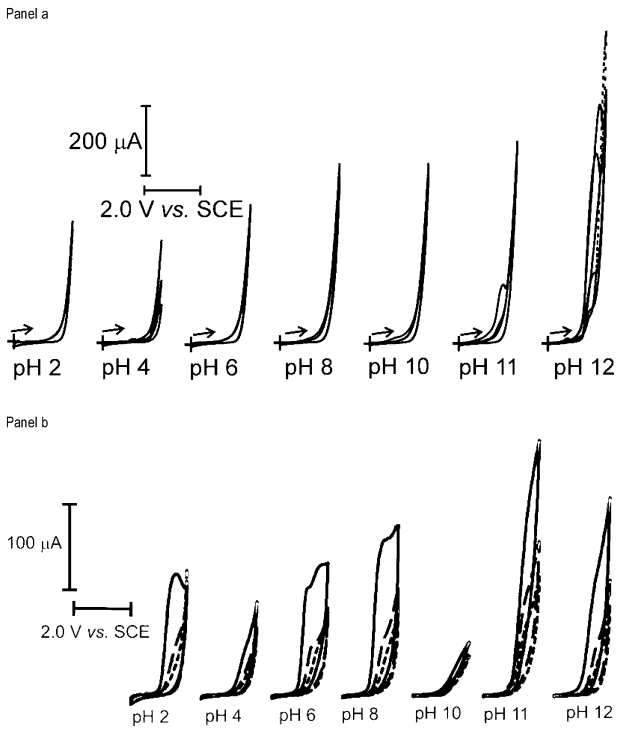

Fig. 1 Cyclic voltammograms (0.1 V s^{-1} scan rate) showing the oxidation of 1.0 nmol Oc_3N immobilised as microdroplets on a 3.0 mm diameter glassy carbon disc electrode immersed in an aqueous electrolyte consisting of (a) 0.1 M sodium perchlorate and 0.1 M phosphate buffer solution, and (b) 0.1 M phosphate buffer solution only, at various values of solution pH. Three consecutive scans are shown in each voltammogram; the peaks observed when the solution pH is <12 are from the third scan. The cross-lines indicate the point of origin, and the arrows show the direction of the initial potential sweep. Note that as a random droplet dispersion is formed in each experiment, the magnitudes of the currents vary.

10 μm, affording droplet coverages of[23b] of *ca.* 0.1, and average inter-droplet distances within the random distribution[23b] of approximately 10 μm. It is readily apparent that when the aqueous bathing medium is at pH values of 11 and below, there is no discernable oxidation wave except that corresponding to solvent breakdown within the potential range studied ($0.0 \leq E/\mathrm{V} \leq 2.0$), the latter occurring at higher potentials than expected on glassy carbon due to the nature of the partially-blocked surface (*q.v.* section 1). In contrast, at pH values of 12 a single, chemically-irreversible oxidation wave appears at 1.7 V *vs.* SCE. This wave is not due to the solvent breakdown; rather it is due to the oxidation of the tertiary amine,[31] presumably at the three-phase boundary of oil|aqueous electrolyte|electrode.[21,22] A plausible mechanism is as follows. Note that all of the Oc_3N is *assumed* to be present within a liquid deposit; we note, but do not discuss, the possibility of surface-adsorbed Oc_3N playing a rôle.

$$Oc_3N(l) + ClO_4^-(aq) - e^- \rightarrow Oc_3N^{+\bullet}ClO_4^-(l) \quad (3a)$$

$$Oc_3N^{\bullet +}ClO_4^-(l) \rightarrow Oc_2N(^{\bullet}CH(CH_2)_6CH_3)(l) + H^+(aq) + ClO_4^-(aq) \quad (3b)$$

$$Oc_2N(^{\bullet}CH(CH_2)_6CH_3)(l) + ClO_4^-(aq) - e^- \rightarrow [Oc_2N^+{=}CH(CH_2)_6CH_3]ClO_4^-(l) \quad (3c)$$

The first step in this process is thought to form the cation radical of trioctylamine. However, in order to maintain an electrostatically-neutral oil phase, this is likely to be accompanied with the insertion of aqueous perchlorate ions (the most lipophilic anion in the aqueous medium). The cleavage of an α-carbon–hydrogen bond with expulsion of protons and perchlorate ions from the oil phase enables the irreversible formation of a radical intermediate, which may undergo further heterogeneous oxidation at lower potentials (*viz.* $E^0_{\mathrm{eqn\ (3a)}} > E^0_{\mathrm{eqn\ (3c)}}$). The dynamics of the oxidation are complex, as evident by the positively-shifted waves in the second and third scans; the formation of new phases during the electrochemical oxidation cannot be discounted. This suggested oxidative pathway may only occur if the trioctylamine exists in a non-protonated state; below the biphasic pK_a of the oil, protonation of the surface is likely,[32] and forms an ion pair:

$$Oc_3N(l) + ClO_4^-(aq) + H^+(aq) \rightleftharpoons Oc_3NH^+ClO_4^-(l) \quad (3d)$$

The extent to which the above ionic surfactant-forming process occurs in the oil phase will depend on the diffusivity of protons and perchlorate ions within the hydrophobic bulk phase, and the degree at which this ionic liquid is soluble in water. As the former is likely to be slow,[33] and the ionic liquid is likely water-insoluble,[34] we suggest this is restricted to an outer "shell".[33] Accordingly, biphasic voltammetry of this protonated phase (as evidenced by the peaks in the third voltammetric scan, presumably oxidising the products of initial electrolysis) may either be initiated along the same triple phase junction, or at the electrode|protonated oil|non-protonated oil boundary. The former case is likely thermodynamically slow; the latter is kinetically limited by perchlorate ion penetration into the bulk coupled with appropriate ion-adjustment in the outer covering.

It is noteworthy that the above reaction mechanisms involve perchlorate ions to exist within the oil phase as well as in the bathing aqueous medium. The above stepwise processes are suggested, over the alternative of proton-coupled electron transfer, since perchlorate ions are hydrophobic and are known to form tight ion pairs.[35] Moreover, when the voltammetry is undertaken in the absence of perchlorate ions (*viz*. in phosphate buffer solutions only), voltammetric peaks are observed between 1.0 and 1.2 V *vs*. SCE at *every* pH value in the range $2.0 \leq \mathrm{pH} \leq 12.0$ (*q.v*. Fig. 1(b)), with broad peaks observed at pH values <4, and two waves above pH 4. At all pH values, the integrated charge reveals that up to up to three electrons can be passed at low scan rates (0.02 V s^{-1}), whilst at higher scan rates, only 1/2 Faraday mol^{-1} can be electrolysed. This more complex voltammetry (which demonstrates an appreciable shift to more negative values as the proton concentration is reduced) can be tentatively understood as being proton release upon electron transfer; quantification is difficult due to the broadness of the waves. Nevertheless, we suggest that since the counter ions are hydrophilic, only the surface of the liquid is protonated, and this charge is countered by the formation of a double layer around the droplets in the aqueous phase. This is perfectly plausible due to the high Gibbs transfer energy for PO_4^{3-}, HPO_4^{2-} and $H_2PO_4^-$. Scheme 1 is a cartoon representation of the fully protonated and deprotonated droplets. For the protonated interface, and for a non-restricted aqueous system, the interfacial charge, σ, can be deduced in the absence of specific adsorption, assuming the surfacial proton activity is related to that in bulk solution

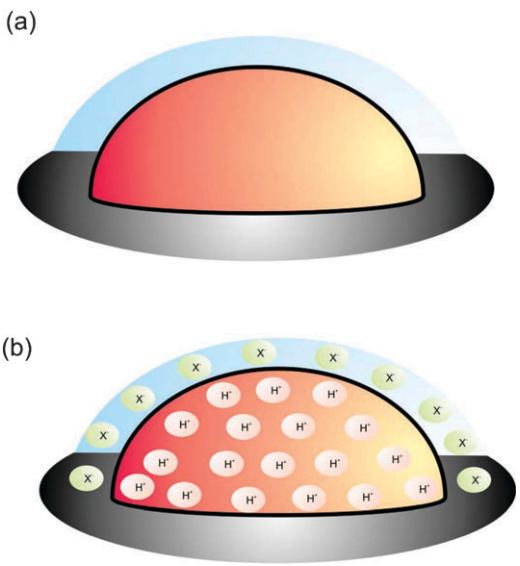

Scheme 1 Cartoon illustration of an oil deposit (orange-yellow) immobilised on an electrode surface (grey) immersed into aqueous electrolyte (blue). Note that in the fully deprotonated case (panel a) there is no specific requirement for local structuring of the electrolyte at the liquid|liquid interface. This is in contrast with panel b for the protonated case, where only the first part of the electrical double layer at the liquid|liquid interface is shown. Note that in this latter case, the degree of association between the protonated oil and the aqueous counterion (X^-) is considered here to be weak; it may be stronger depending on the nature of the counterion (see text).

via a Boltzmann distribution of the electrostatic surface potential,[7] $\chi = \chi_{\mathrm{surf}} - \chi_{\mathrm{aq\ bulk}}$:

$$\sigma = \frac{q_0 \Gamma_{\mathrm{oil^{Red}}}}{1 + \left(K_{\mathrm{a}}^{\mathrm{biphasic}} / a_{\mathrm{H^+}}^{\mathrm{bulk}}\right) \exp(q_0 \chi / k_{\mathrm{B}} T)} \qquad (4)$$

In the above, $\Gamma_{\mathrm{oil^{Red}}}$ is the total surface concentration of protonation sites, *viz*. $\Gamma_{\mathrm{oil^{Red}}} = \Gamma_{\mathrm{AH^+}} + \Gamma_{\mathrm{A}}$. Although the surface charge is deducible from the differential capacity, C_{d}, since $C_{\mathrm{d}} = \partial\sigma/\partial E$, the latter is difficult to estimate reliably from the voltammetric data presented in Fig. 1, not least due to the difficulties in obtaining perfectly reproducible droplet array distributions.

3.2 Voltammetry of $Ru(bpy)_3^{2+}$ at glassy carbon electrodes

Fig. 2 illustrates cyclic voltammograms (at a scan rate of 0.1 V s^{-1}) for the oxidation of 1.0 mM tris(2,2′-bipyridyl)-ruthenium(II) in aqueous solution at a "naked" glassy carbon electrode at various solution pH values. It is evident that at low pH, a single, electrochemically quasi-reversible wave at $E_{\mathrm{mid}} = 1/2(E_{\mathrm{p}}^{\mathrm{Ox}} + E_{\mathrm{p}}^{\mathrm{Red}}) = 1.03 \pm 0.01$ V *vs*. SCE ($\Delta E_{\mathrm{pp}} = 83 \pm 7$ mV; $i_{\mathrm{p}}^{\mathrm{Ox}}/i_{\mathrm{p}}^{\mathrm{Red}} = 1.2 \pm 0.1$) is present. This one-electron wave is due to the following redox process.[29]

$$\mathrm{Ru(bpy)_3^{2+}(aq)} - \mathrm{e^-} \rightleftharpoons \mathrm{Ru(bpy)_3^{3+}(aq)} \qquad (5)$$

A Randles–Sevcík analysis of the peak oxidative current furnished a diffusion coefficient of $Ru(bpy)_3^{2+}$ of $5.7 \pm 1.4 \times 10^{-6}$ cm^2 s^{-1}. When the solution pH is larger than *ca*. pH 5, a voltammetric pre-wave at $E_{\mathrm{p}}^{\mathrm{Ox}} = 0.83$ V *vs*. SCE becomes discernable. This feature dominates the voltammetry at high scan rates, and increases in magnitude with prolonged immersion of the electrode in the aqueous solution (data not shown). It has been demonstrated[36] that this wave is due to the voltammetry of adsorbed $Ru(bpy)_3^{2+}$ which is irreversibly "stripped" off the electrode during oxidation.

3.3 Biphasic electron transfer

The presence of microdroplets of Oc_3N on the surface of the glassy carbon electrode causes the oxidation peak of $Ru(bpy)_3^{2+}$ to increase in magnitude compared with bare electrode *despite the reduced electrode area for the oxidation*—see Fig. 3 for representative voltammograms. Strikingly, these cyclic voltammograms do not exhibit reverse waves for the

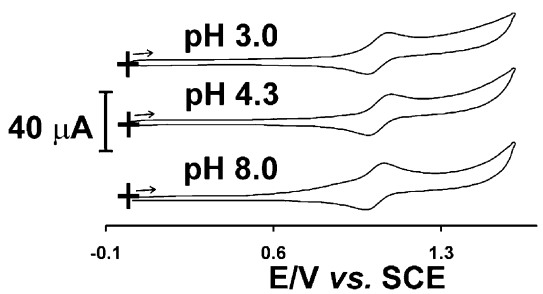

Fig. 2 Cyclic voltammograms (0.1 V s^{-1} scan rate) for the oxidation of 1.0 mM $Ru(bpy)_3^{2+}$ at a 3.0 mm diameter glassy carbon electrode immersed in 0.1 M aqueous phosphate buffer solution. Only one voltammetric scan is shown. The cross-lines indicate the point of origin, and the arrows show the direction of the initial potential sweep.

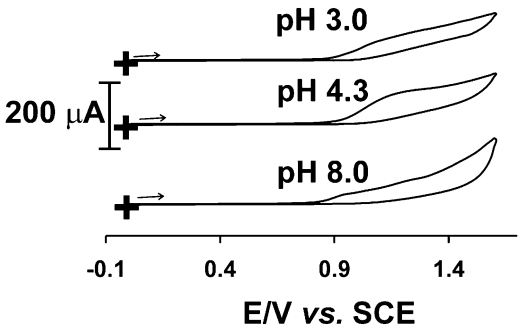

Fig. 3 Cyclic voltammograms (0.1 V s^{-1} scan rate) for the oxidation of 1.0 mM $Ru(bpy)_3^{2+}$ at a 3.0 mm diameter glassy carbon electrode on which 1.0 nmol Oc_3N are immobilised in the form of microdroplets, and immersed in 0.1 M aqueous phosphate buffer solution. Only one voltammetric scan is shown. The cross-lines indicate the point of origin, and the arrows show the direction of the initial potential sweep.

reduction of electrogenerated $Ru(bpy)_3^{3+}$, suggestive of its reduction at the oil|aqueous interface:

$$Ru(bpy)_3^{3+}(aq) + oil^{Red}(l) \rightarrow Ru(bpy)_3^{2+}(aq) + oil^{Ox}(l) \quad (6)$$

This amperometric augmentation of the oxidation wave of the aqueous complex occurs at every value of the solution pH within the range tested. However, it observes a pH dependence similar to that reported for the voltammetry of the oil (*q.v.* section 3.1), see Fig. 3. UV/visible spectrophotometric investigations of mixtures of aqueous $Ru(bpy)_3^{3+}$ with Oc_3N suggested that no partitioning of either species into oil or aqueous phases, suggesting that eqn (6) is truly a biphasic electronation event.

In order to determine whether this liquid|liquid redox catalysis is accompanied with luminescence, the electrochemical oxidation perturbation was limited as a pulse by potentiostatting the droplet-modified electrode at 1.2 V *vs.* SCE for 20 s. This potential allows for the formation of $Ru(bpy)_3^{3+}$ under mass-transport-limited conditions. Fig. 4 illustrates typical ECL responses.‖ It is evident that the ECL response is instantaneous with formation of $Ru(bpy)_3^{3+}$, attaining steady-state (except at higher values of solution pH) within a few seconds. Although chronoamperometric transients were recorded, these are of little value for this preliminary work since at certain solution pH values, these also contain information regarding the oxidation of the oil (*q.v.* section 3.1). ECL occurs at every pH value in solution examined, with the ECL intensity being greatest for solution pH values in strongly alkaline media (pH > 10), and smallest when the aqueous phase is of low pH; plots of the ECL signal intensity (the initial spike, or the steady-state value) against pH are illustrated in Fig. 5. The slight discontinuity observed in these semi-logarithmic plots is a marker for the biphasic pK_a as it indicates a change in the mechanism of ECL production: above the interfacial pK_a, $Ru(bpy)_3^{3+}$ reacts with neutral trioctylamine, with electron transfer presumably occurring in concert with ion transfer (*viz.* perchlorate ion insertion or

‖ Although the ECL signal intensity is reported herein as being of millivolt units, this is the signal recorded by the photodiode employed; a reviewer has noted that the SI unit of light intensity is the candela.

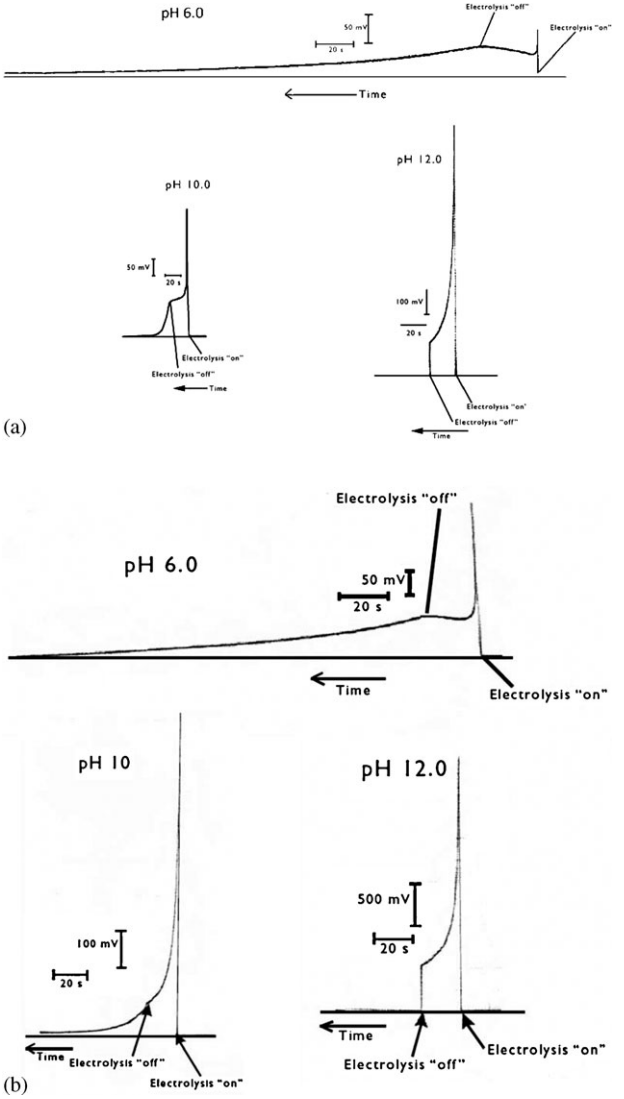

Fig. 4 ECL transients (signal *vs.* time) obtained under a single stepped potential electrolysis (see text for parameters). The 3.0 mm diameter glassy carbon working electrode was modified with 1.0 nmol Oc_3N microdroplets and immersed into an aqueous solution containing 1.0 mM $Ru(bpy)_3^{2+}$. Panel (a) is for a solution containing only 0.1 M phosphate buffer solution; panel (b) exhibits representative data when the aqueous solution contains both 0.1 M sodium perchlorate and 0.1 M phosphate buffer solution.

proton expulsion) across the interface; below the heterogeneous pK_a, electron transfer across the liquid|liquid interface is apparently sluggish. Extrapolating as suggested from the data in Fig. 5 suggests that the biphasic pK_a for this system is roughly between 9.7 and 10.8 (when perchlorate ions are absent or present in the aqueous phosphate buffer solution). These approximate values are reasonable estimates. We next explore the ECL transient data further.

The presence of perchlorate ions in the bathing aqueous medium exhibit a surprisingly large effect on the observed ECL magnitude; ECL signals are apparently greater when these ions exist in aqueous solution. We suggest this reflects the kinetics of the ion-coupled electron transfer process, but also, noting previous work by Bard regarding the distinct

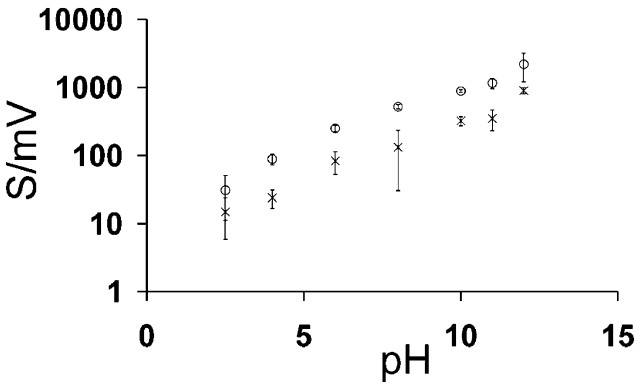

Fig. 5 Plots of the maximal ECL signal intensity (S) as a function of the solution pH, when the aqueous solution contains 0.1 M phosphate buffer (×), or 0.1 M sodium perchlorate with 0.1 M phosphate buffer (○). Note that the ordinate axis is logarithmic. The points plotted are average data, with the standard deviation marking the error bars.

effect of halides on ECL intensity, potentially due to ionic stabilisation of the transition state.[37] Under strongly alkaline solution conditions, the following processes are plausible.

$$\mathrm{Ru(bpy)_3^{3+}(aq) + Oc_3N(l) + ClO_4^-(aq)} \rightarrow \mathrm{Oc_3N^{+\bullet}ClO_4^-(l) + Ru(bpy)_3^{2+}*(aq)} \rightarrow h\nu + \mathrm{Ru(bpy)_3^{2+}(aq) + Oc_3N^{+\bullet}ClO_4^-(l)} \quad (7a)$$

$$\mathrm{Ru(bpy)_3^{3+}(aq) + Oc_3N(l)} \rightarrow \mathrm{Oc_3N^{+\bullet}(l) + Ru(bpy)_3^{2+}*(aq)} \rightarrow h\nu + \mathrm{Ru(bpy)_3^{2+}(aq) + Oc_3N^{\bullet}(l) + H^+(aq)} \quad (7b)$$

The further oxidation of the oil product can take place both at the solid electrode, or across the liquid|liquid interface. The reaction in the presence of perchlorate ions merely requires these to transfer and ion-pair from the aqueous phase as the organic oil is oxidised, to preserve the electroneutrality of the organic phases. In contrast, as hydroxide and phosphate are highly hydrophilic, we suggest charge-compensation by ion-pair association at the interface. The alternative explanation of $Oc_3N^{+\bullet}$ "expulsion" from the oil phase cannot be ruled out. Note that in the above, although it is suggested that ion-coupled electron transfer occurs in one case and not the other, these may not be actual precise mechanisms. In any case, it is clear that the reactions yield different products, meaning that the overall reaction driving force is different in each case. This will affect the ECL signal intensity.

Below the biphasic pK_a, the following mechanisms are possible.

$$\mathrm{Ru(bpy)_3^{3+}(aq) + Oc_3NH^+ClO_4^-(l)} \rightarrow \mathrm{H^+(aq) + Oc_3N^{+\bullet}ClO_4^-(l) + Ru(bpy)_3^{2+}*(aq)} \rightarrow h\nu + \mathrm{Ru(bpy)_3^{2+}(aq) + Oc_3N^{+\bullet}ClO_4^-(l) + H^+(aq)} \quad (8a)$$

$$\mathrm{Ru(bpy)_3^{3+}(aq) + Oc_3NH^+(l)} \rightarrow \mathrm{H^+(aq) + Oc_3N^{+\bullet}(l) + Ru(bpy)_3^{2+}*(aq)} \rightarrow h\nu + \mathrm{Ru(bpy)_3^{2+}(aq) + Oc_3N^{\bullet}(l) + 2H^+(aq)} \quad (8b)$$

The first process can occur at the liquid|liquid interface. The last can only occur at a distance from the interface (the outer Helmholz plane equivalent). In the light of the Marcus expressions (eqns (F2)), it is apparent that the reduced ECL signal in the absence of the perchlorate anion likely stems from a reduced pre-exponential factor (as both processes involve proton-coupled electron transfer), due to the large separation of reactants, resulting from the incorporation of a "long-range tunnel factor". As in the preceding paragraph, the changes in the overall driving force as a result of the two different mechanisms cannot be assumed to be negligible, since the intrinsic barrier additionally reflects a proton reorganization energy.[19b,38,39] Moreover, the possibility of eliciting sub-surface oil oxidation *via* long-range electron transfer coupled with proton transfer in the second mechanism (eqn (8b)) cannot be discounted as being a viable. As in the case of the alkaline solution, the products of the proposed biphasic reaction may be oxidised further both at the solid electrode and at the liquid|liquid interface. The latter pathway may be the underlying cause of the increase in ECL signal intensity during the 20 s electrolysis as noticed in the low pH data reported in Fig. 4. Alternative mechanisms such as two-electron oxidations to form Ru^{I} species, which may yield ECL *via* comproportionation with Ru^{III} species, or *via* excited-state quenching by Oc_3N,[40] cannot be discounted.

It thus appears that ECL at liquid|liquid microinterfaces is highly sensitive to the chemical nature of the interface, and appears to be suited to the measurement of heterogeneous pK_a. It is insightful to enquire whether this droplet-modified system is able to afford any quantitative kinetics information, or even of the interfacial concentrations of protonated *versus* deprotonated amines as a function of aqueous pH. The shape of the ECL transients illustrated in Fig. 4 suggests there is a solution pH-dependent response in the cessation of ECL when the electrochemical perturbation is removed: at high pH values, ECL cessation is apparently instantaneous (within the accuracy of the recording equipment); in acidic solutions, there is a slow, first-order decay of the ECL signal. Extraction of the first-order decay constant (k) reveals a pH dependence

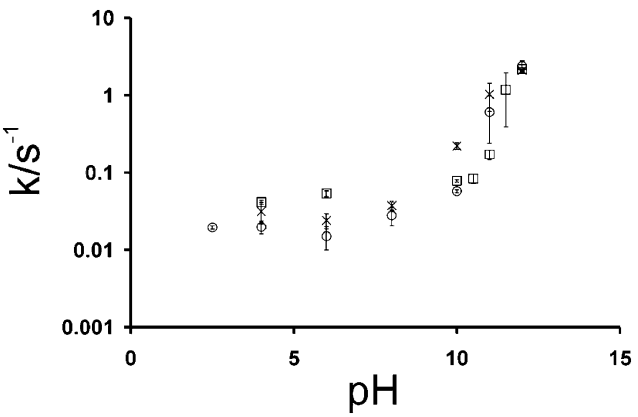

Fig. 6 Plots of the observed first-order ECL decay constant (k) as a function of the solution pH. The solution contains 0.1 M phosphate buffer (×), or 0.01 M phosphate buffer (□), or 0.1 M sodium perchlorate and 0.1 M phosphate buffer (○) Note that the ordinate axis is logarithmic. The points plotted are average data, with the standard deviation marking the error bars.

Table 1 Variation in the decay constant in the presence of a varied concentration of $Ru(bpy)_3^{2+}$(aq) with 1.0 nmol Oc_3N immobilised on the working electrode

$[Ru(bpy)_3^{2+}]$/M	pH	$k_{average}/s^{-1}$
1.0	8.0	0.06 ± 0.01
1.0	10.0	0.09 ± 0.01
1.0	12.0	2.25 ± 0.08
2.0	8.0	0.05 ± 0.01
2.0	10.0	0.10 ± 0.02
2.0	12.0	2.35 ± 0.23

illustrated in Fig. 6. Similar values for k were obtained when the concentration of aqueous Ru^{II} were doubled (*q.v.* Table 1). Doubling the amount of Oc_3N on the surface had no significant effect on the values of k reported (data not shown); this variable causes the a change in the surface availability of Oc_3N at the expense of reduced amount of coverage for solid|liquid heterogeneous electron transfer. The differences between the plots for aqueous ionic media likely stem from the enhanced interfacial conductivity discussed earlier when perchlorate ions are present in aqueous solution; the presence of electrical double layers ensure that electron transfer occurs over longer distances, so becomes slower and, correspondingly, more difficult to measure accurately. Nevertheless, such plots directly enable the extraction of the biphasic pK_a, which is found to be 10.7 when perchlorate ions are present (at 0.1 M concentration) in the aqueous phase and 10.2 when the aqueous phase is merely phosphate buffer solution (at 0.1 M concentration). These values compare well with those reported *via* the measurement of the ECL signal intensity, although, these values are also merely estimates as they are extracted *via* reaction kinetics and have not been corrected for mass transport rates. The latter can be given by a Smoluchowski manner (where we have ignored convective effects): $\frac{1}{k} = \frac{1}{k^{true}_{electron\ transfer}} + \frac{1}{k_{diffusion}} + \frac{1}{k_{migration}}$.

Reducing the concentration of the phosphate buffer solution by an order of magnitude to 0.01 M effectively *increases* the apparent biphasic pK_a to 10.9 (see Fig. 6). This is consistent with the perceived view that by increasing the size of the solution-phase double layer by reducing its ionic strength causes electron-transfer to occur over larger distances, demonstrating that the ECL experiment is sensitive to interfacial structure and activity effects. However, the whole picture is further complicated by anion association effects, as suggested for the case in the presence of perchlorate ions, and the possibility of diffusion–migration of the electrogenerated Ru^{III} species occurring within the solution phase in the droplet-centred electrical double layer, under conditions of full protonation of the liquid|liquid interface cannot be neglected.

To understand the reason for the non-instantaneous ECL decay, consider the following approximation of the reaction mechanisms, where we also include a non-radiative (NR) decay; note we exclude third-body effects in the latter route.

$$Ru^{III}(aq) + oil^{Red}(l) \underset{k_{-1}}{\overset{k_1}{\rightleftharpoons}} oil^{Ox}(l) + Ru^{II}*(aq) \quad (9a)$$

$$Ru^{II}*(aq) \xrightarrow{k_2} h\nu + Ru^{II}(aq) \quad (9b)$$

$$Ru^{II}*(aq) \xrightarrow{k_{NR}} Ru^{II}(aq) \quad (9c)$$

Application of the steady-state hypothesis to $Ru(bpy)_3^{2+}*$ (ignoring the transport-based loss of the ruthenium species from the droplet-modified interface) results in the following expression for the ECL signal intensity (S):

$$S \propto k_2[Ru^{II}*] \approx \phi k_1[Ru^{III}]\Gamma_{oil^{Red}} \quad (10)$$

where ϕ is the quantum yield of the ECL ($\phi = k_2/(k_2 + k_{NR})$), and the reverse electron transfer is assumed to be kinetically pathological, *viz.* $k_{-1}\Gamma_{oil^{Ox}} \ll k_2 + k_{NR}$. Since the ECL signal measures the decay of the excited state, the associated rate constant (k_2) is, under the approximation of negligible ionic strength effects, and ignoring environmental influences, independent of the solution pH. This means that the observed decay stems from the pH-dependent bimolecular reaction kinetics at the liquid|liquid interface. With the cessation of electrolysis, Ru^{III} is no longer regenerated after its reaction

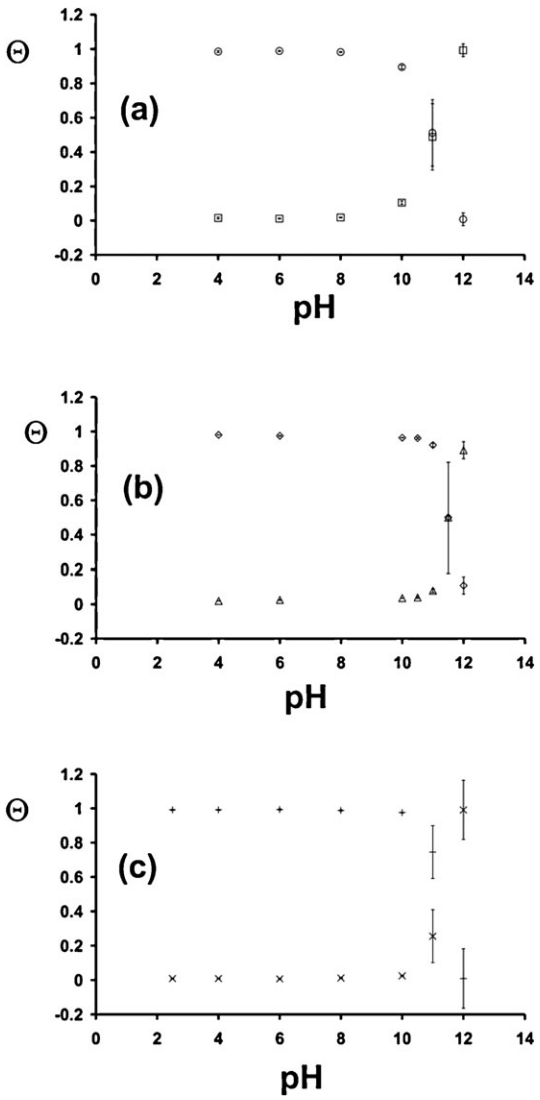

Fig. 7 Plots illustrating the fractional surface concentration (Θ) of protonated (AH^+) and (Θ) deprotonated (A) Oc_3N. (a) 0.1 M phosphate buffer solution, (□) Θ_A, (○) Θ_{AH^+}; (b) 0.01 M phosphate buffer solution, (△) Θ_A, (◇) Θ_{AH^+}; (c) 0.1 M sodium perchlorate with 0.1 M phosphate buffer solution, (×) Θ_A, (+) Θ_{AH^+}. The points plotted are average data, with the standard deviation marking the error bars.

with the oil, causing the observed pseudo-first-order signal decay, given the independence of the rate constant on the aqueous Ru^{II} species concentration, *viz.* $k = \phi k_1 \Gamma_{oil^{Red}}$. The pH-dependence thus merely reflects the slow kinetics of the liquid|liquid proton-coupled electron transfer at low solution pH, and its mechanism change when the surface is fully deprotonated. Although it is not possible to determine the activation free energy for this reaction, unless drastic approximations are made, it is possible to calculate the fraction of the interface that is protonated at each value of the solution pH, thereby determining a true, thermodynamic value of the biphasic pK_a using the values extracted from the kinetics measurements. Assuming that the most acidic conditions employed herein corresponds to a fully protonated interface (and so has a first order decay constant of k_{AH^+}), that observed at the most alkaline (solution pH 12.0) corresponds to a fully deprotonated interface (with first-order decay constant of k_A), and that increases in the observed kinetics of the decay results from the linear combination of kinetics due to fast reaction between deprotonated oil and the electrogenerated oxidant, the fraction of deprotonated amine can be deduced by solving the following quadratic expression, estimating activity coefficients using the extended version of the Debye–Hückel Law (*viz.* $\lg(f_{H^+}) = (-0.5\sqrt{I})/(1 + \sqrt{I})$), noting that aqueous phosphoric acid has the following acid association constants[41] at 298 K: pK_{a1} = 2.15, pK_{a2} = 7.20, pK_{a3} = 12.35).**

$$k = k_A \Theta_A + \left(\frac{k_{AH^+} f_{H^+}}{K_a^{biphasic} / \Gamma_{oil^{Red}}} \right) \Theta_A^2 \qquad (11)$$

In this way, noting that $\Theta_{AH^+} + \Theta_A = 1$, the plots given in Fig. 7 can be constructed by solving eqn (11), using the estimated biphasic pK_a values obtained from Fig. 6 as an initial guess of the true heterogeneous pK_a, a new value for this pK_a can be obtained when $\Theta_{AH^+} + \Theta_A = 0.5$. Use of this value allows for successive, iterative refinement of the surfacial pK_a.††

** The observed decay constant, k, is assumed to be split as follows.

$$k = k_{AH^+}^{eff} + k_A^{eff}$$

$$\Rightarrow k = k_{AH^+}^{true} \Gamma_{AH^+} + k_A^{true} \Gamma_A$$

$$\Rightarrow k = k_{AH^+}^{true} \frac{\Gamma_A^2}{K_a^{biphasic}} f_{H^+} + k_A^{true} \Gamma_A$$

$$\Rightarrow k = \frac{k_{AH^+} f_{H^+}}{K_a^{biphasic}} \Theta_A \Gamma_A + k_A \Theta_A$$

Eqn (11) follows from this.

†† Eqn (11) also requires the assumption of the surface concentration of redox sites, Γ_{oil}^{Red}. The experimental data were undertaken using 1.0 nmol of Oc_3N. It is not unreasonable to assume the droplets are hemispherical and uniformly distributed and with an average size (r_0) of 10 μm.[23] Given that the density[42] of Oc_3N is 0.81 g cm^{-3} at 298 K, undiluted Oc_3N exhibits a concentration of 2.3 M, and suggests that the number of droplets on the electrode is on the order of 210. Further assuming that the surface concentration in a thin outer "shell", of thickness d, and thus volume of $2\pi r_0 d$ (ignoring terms in d^2 and higher). The shell thickness may be calculated by first estimating the self diffusion coefficient of Oc_3N using the Wilke–Chang expression[43] (assuming a viscosity[42] of 15 cP and association parameter of 1, followed by the Stokes–Einstein expression to determine the "radius" (r_1) of Oc_3N. d follows by noting $d = 2r_1$. Accordingly, $\Gamma_{oil^{Red}} = 1.1 \times 10^{-10}$ mol cm^{-2}. This is, satisfyingly, on the order of magnitude anticipated.

It is evident that these "activity-corrected" biphasic pK_a determination plots vary little (within experimental error) on the ionic media: the estimated biphasic pK_a values are 11.2 ± 0.1 (in 0.1 M phosphate buffer solution), 11.5 ± 0.1 (in 0.01 M phosphate buffer solution), and 11.3 ± 0.1 (in 0.1 M phosphate buffer solution containing 0.1 M sodium perchlorate). At the biphasic pK_a, the surface electrostatic potential should be zero. This latter term is readily determined using eqn (12), which merely equates both approximations employed for the surface proton activity in section 1.

$$\chi = -\frac{k_B T}{q_0} \{ \ln(\Theta_A \Gamma_{oil^{Red}} f_{H^+}) + 2.303 \mathrm{pH} \} \qquad (12)$$

The data (based on the average computed values given above) are provided in Table 2, and suggest that $\chi = 0$ when the aqueous solution pH is 10.8 (if it is composed of 0.1 M phosphate buffer solution), 10.9 (if the concentration of the phosphate buffer is 0.01 M) and 11.0 (if the electrolyte is 0.1 M phosphate buffer solution with 0.1 M sodium perchlorate added). These values are all in good agreement with the estimated biphasic pK_a, testifying to the validity of the use of activity coefficient approximation detailed above.

Since the ECL signal depends on the surface concentration as suggested by eqn (10), experiments were undertaken in which the oil microdroplet phase consisted of the tertiary amine dissolved in an organic solution. Two solvents were considered: *n*-octane, and benzonitrile. These were chosen given there are perceived differences in their interfacial structure.[18] Experiments were conducted as before, employing only phosphate buffer solutions, and the first-order decay of the ECL signal at the end of electrolysis was treated to determine the first order rate constant. Fig. 8 illustrates the dependence of this on the relative composition of the oil mixture. It is apparent that above the biphasic pK_a, as the droplets are diluted, the reaction rate decreases, as anticipated given the reduced surfacial concentrations of the redox species. Moreover, comparison of the two solvents clearly demonstrates that the reaction kinetics are slowed as the interfacial hydrogen-bonding weakens.[18] This distance-dependent electron transfer is not wholly unexpected. In contrast, below the biphasic pK_a, the reaction kinetics apparently increase as the oil phase is diluted with inert solvent, even though the magnitude of these kinetics is smaller than in the strongly

Table 2 Dependence of the calculated electrostatic surface potential (χ) using eqn (12) on the solution pH

pH	χ^a/V	χ^b/V	χ^c/V
2.5	n/a[d]	n/a[d]	0.58
4.0	0.47	0.46	0.49
6.0	0.36	0.33	0.38
8.0	0.23	n/a[d]	0.24
10.0	0.07	0.09	0.11
10.5	n/a[d]	0.06	n/a[d]
11.0	−0.03	0.01	−0.01
11.5	n/a[d]	−0.06	n/a[d]
12.0	−0.11	−0.11	−0.11

[a] 0.1 M phosphate buffer solution. [b] 0.01 M phosphate buffer solution. [c] 0.1 M sodium perchlorate + 0.1 M phosphate buffer solution. [d] n/a = Not measured.

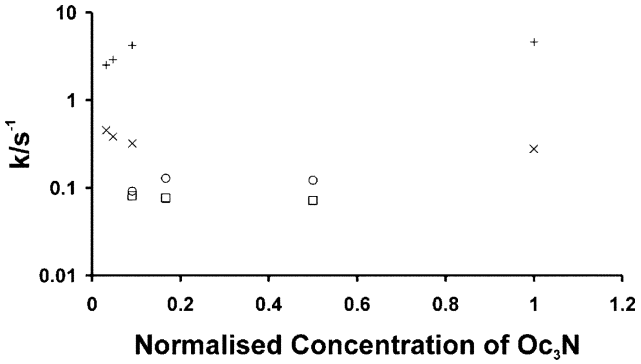

Fig. 8 Plots illustrating the dependence of the first-order ECL decay constant with the normalised concentration of Oc_3N (calculated noting that a normalised concentration of 1.0 corresponds to an Oc_3N concentration of 2.3 M) present in the microdroplets (see text). In all cases the solution pH merely consisted of 0.1 M phosphate buffer solution; ECL data were obtained using a 3.0 mm diameter glassy carbon disc electrode coated with 1.0 nmol Oc_3N microdroplets and immersed into the above aqueous solution containing 1.0 mM $Ru(bpy)_3^{2+}$. Key: (×) octane solvent, solution phase at pH 10; (+) octane solvent, solution phase at pH 12; (□) benzonitrile solvent, solution phase at pH 10; (○) benzonitrile solvent, solution phase at pH 12. Note that the axis scale is logarithmic.

alkaline solution case. If the ECL signal is *via* proton-coupled electron transfer from the biphasic surface alone, then these data trends may be understood by enhanced surface concentrations of the amine *cf.* bulk droplet solution, presumably driven by the minimisation of the interfacial tension by protonation: the increased hydrogen bonding that this affords may cause a large structure over which electron transfer occurs, causing the latter process to be less efficient. This is not unreasonable given similar suggestions of self-assembly at liquid|liquid interfaces by Compton[23] and Girault.[44] Nevertheless, any competition between slow proton-coupled electron transfer at the biphasic interface and faster long-range outer-sphere electron transfer between the aqueous phase and the bulk droplet solution cannot be ruled out.

Conclusions

ECL at droplet-modified electrodes has been demonstrated, and has been employed to extract information regarding the molecular structure of the oil|aqueous interface, and thus its heterogeneous pK_a, under appropriate assumptions. The biphasic pK_a for interfacial trioctylamine appears to be *ca.* 11. This is satisfyingly close to values previously reported for *n*-octylamine and dioctylamine (10.65 and 11.01, respectively at 298 K) and dihexylamine (11.01 at 298 K) in ethanol–water mixtures,[45] and of aqueous triethylamine and tripropylamine (10.9 and 10.4, respectively at 298 K).[40] The consistency of these data with those implied by the pH dependence of the cyclic voltammograms of the oil microdroplets is pleasing. In part, the sensitivity of the ECL technique relies on subtleties in the mechanism for the biphasic electron transfer process: above the biphasic pK_a, outer sphere electron transfer occurs; below the biphasic pK_a, proton-coupled electron transfer appears to dominate. This latter process appears to be kinetically sluggish presumably due to a larger reactant separation, augmented intrinsic barrier due to the N–H bond dissociation and proton reorganisation energy, and offset by possible proton tunnelling. Extension of the semi-empirical theories of electron transfer at the liquid|liquid interface[16,17] to encompass the proton-coupled electron transfer[19b,38] is required when convoluted with diffusion-migration mass transport processes for this particular geometry (to account for any effects within the droplet electrical double layer), to extract the relevant physicochemical dynamics responsible for the ECL interfacial kinetics from these data, and to rationalise kinetic isotope effects not detailed herein.

Acknowledgements

C. L.-F. and G. M. G. express gratitude to Hull University for funding *via* the Graduate Teaching Assistance Scheme. IH thanks Selçuk University of Konya for funding her work at Hull University *via* the ERASMUS European Exchange programme. M. J. B. gratefully thanks The Nuffield Foundation for financing his summer studentship *via* their Undergraduate Research Bursary scheme (GR/N URB/33192). J. W. is indebted to Hull University for financial support *via* a start-up grant, and thanks Evangelia Christoforou for undertaking some experiments.

References

1 See, for example: R. P. Bell, *The Proton in Chemistry*, Chapman and Hall, London, UK, 2nd edn, 1973.
2 See, for example: A. G. Marangoni, *Enzyme Kinetics: A Modern Approach*, John Wiley, New York, USA, 2003, pp.79–89.
3 See, for example: K. A. Vincent, A. Parkin and F. A. Armstrong, *Chem. Rev.*, 2007, **107**, 4366.
4 M. Gutman, E. Shimoni and Y. Tsdadia, *Electron and Proton Transfer in Chemistry and Biology*, in *Studies in Physical and Theoretical Chemistry*, eds. A. Müller, H. Ratajczak, W. Junge and E. Diemann, Elsevier, Amsterdam, The Netherlands, 1992, vol. 78, pp. 273–285.
5 E. Bardez, E. Monnier and B. Valeur, *J. Phys. Chem.*, 1985, **89**, 5031.
6 (*a*) C. P. Smith and H. S. White, *Anal. Chem.*, 1993, **65**, 3343; (*b*) T. Sokalski, P. Lingenfelter and A. Lewenstam, *J. Phys. Chem. B*, 2003, **107**, 2443.
7 See for example, (*a*) S. Durand-Vidal, J. P. Simonin and P. Turq, *Electrolytes at Interfaces*, Kluwer Academic, Dordrecht, 2000; (*b*) R. J. Hunter, *Introduction to Modern Colloid Science*, Oxford University Press, Oxford, 2nd edn, 1993.
8 M. Gutman, *Biochim. Biophys. Acta*, 2000, **1458**, 120.
9 For reviews on electroluminescence, see: (*a*) L. R. Faulkner and A. J. Bard, Electrogenerated Chemiluminescence, in *Electroanalytical Chemistry*, ed. A. J. Bard, Marcel Dekker, New York, USA, 1977, vol. 10, p. 1; (*b*) M. M. Richter, *Chem. Rev.*, 2004, **104**, 3003; (*c*) W. Miao, *Chem. Rev.*, 2008, **108**, 2506.
10 C. M. Pharr, R. C. Engström, J. Klancke and P. L. Unzelman, *Electroanalysis*, 1990, **2**, 217.
11 (*a*) S. Szunerits, J. M. Tam, L. Thouin, C. Amatore and D. R. Walt, *Anal. Chem.*, 2003, **75**, 4382; (*b*) C. Amatore, A. Chovin, L. Servant, N. Sojic, S. Szunerits and L. Thouin, *Anal. Chem.*, 2004, **76**, 7202; (*c*) C. Amatore, C. Pébay, L. Servant, N. Sojic, S. Szunerits and L. Thouin, *ChemPhysChem*, 2006, **7**, 1322.
12 A. Chovin, P. Garrigue, P. Vinatier and N. Sojic, *Anal. Chem.*, 2004, **76**, 357.
13 R. P. Van Duyne and S. F. Fischer, *Chem. Phys.*, 1974, **5**, 183.

14 (*a*) Y. Zu, F.-R. Fan and A. J. Bard, *J. Phys. Chem. B*, 1999, **103**, 6272; (*b*) F. Kanoufi, C. Cannes, Y. Zu and A. J. Bard, *J. Phys. Chem. B*, 2001, **105**, 8951.
15 (*a*) J. Zhang and P. R. Unwin, *J. Chem. Soc., Perkin Trans. 2*, 2001, 1608; (*b*) J. Zhang and P. R. Unwin, *Phys. Chem. Chem. Phys.*, 2002, **4**, 3820; (*c*) F. Li, A. Whitworth and P. R. Unwin, *J. Electroanal. Chem.*, 2007, **602**, 70.
16 (*a*) R. A. Marcus, *J. Phys. Chem.*, 1990, **94**, 1050; (*b*) R. A. Marcus, *J. Phys. Chem.*, 1990, **94**, 4152; (*c*) Addendum: R. A. Marcus, *J. Phys. Chem.*, 1990, **94**, 7742; (*d*) R. A. Marcus, *J. Phys. Chem.*, 1991, **95**, 2010.
17 G. Geblewicz and D. J. Schiffrin, *J. Electroanal. Chem.*, 1988, **244**, 27.
18 (*a*) K. Kashimoto, J. Yoon, B. Y. Hou, C. H. Chen, B. H. Lin, M. Aratono, T. Takiue and M. L. Schlossman, *Phys. Rev. Lett.*, 2008, **101**, 076102; (*b*) G. Luo, S. Malkova, S. V. Pingali, D. H. Schultz, B. H. Lin, M. Meron, T. J. Graber, J. Gebhardt, P. Vanýsek and M. L. Schlossman, *Faraday Discuss.*, 2005, **129**, 23; (*c*) M. A. Leich and G. L. Richmond, *Faraday Discuss.*, 2005, **129**, 1.
19 (*a*) H. M. V. Huynh and T. J. Meyer, *Chem. Rev.*, 2007, **107**, 5004; (*b*) C. Costentin, *Chem. Rev.*, 2008, **108**, 2145.
20 See, for example: L. Dennany, C. F. Hagan, T. E. Keynes and R. J. Forster, *Anal. Chem.*, 2006, **78**, 1412.
21 (*a*) C. E. Banks, T. J. Davies, R. G. Evans, G. Hignett, A. J. Wain, N. S. Lawrence, J. D. Wadhawan, F. Marken and R. G. Compton, *Phys. Chem. Chem. Phys.*, 2003, **5**, 4053; (*b*) F. Scholz, U. Schröder and R. Gulaboski, *Electrochemistry of Immobilised Particles and Droplets*, Springer, Heidelberg, Berlin, Germany, 2005.
22 (*a*) K. Aoki, P. Tasakorn and J. Y. Chen, *J. Electroanal. Chem.*, 2003, **542**, 51; (*b*) N. Katif, S. M. MacDonald, A. M. Kelly, E. Galbraith, T. D. James, A. T. Lubben, M. Opallo and F. Marken, *Electroanalysis*, 2008, **20**, 469; (*c*) K. Charreteur, F. Quentel, C. Elleouet and M. L'Her, *Anal. Chem.*, 2008, **80**, 5065.
23 (*a*) B. A. Brookes, T. J. Davies, A. C. Fisher, R. G. Evans, S. J. Wilkins, K. Yunus, J. D. Wadhawan and R. G. Compton, *J. Phys. Chem. B*, 2003, **107**, 1616; (*b*) T. J. Davies, B. A. Brookes, A. C. Fisher, K. Yunus, S. J. Wilkins, P. R. Greene, J. D. Wadhawan and R. G. Compton, *J. Phys. Chem. B*, 2003, **107**, 6431; (*c*) T. J. Davies, B. A. Brookes and R. G. Compton, *J. Electroanal. Chem.*, 2004, **566**, 193; (*d*) T. J. Davies, A. C. Garner, S. G. Davies and R. G. Compton, *J. Electroanal. Chem.*, 2004, **570**, 171; (*e*) F. G. Chevallier, T. J. Davies, O. V. Klymenko, L. Jiang, T. G. J. Jones and R. G. Compton, *J. Electroanal. Chem.*, 2005, **580**, 265; (*f*) T. J. Davies, A. C. Garner, S. G. Davies and R. G. Compton, *ChemPhysChem*, 2005, **6**, 2633.
24 C. Amatore, A. Olenick and I. B. Svir, *J. Electroanal. Chem.*, 2005, **575**, 103.
25 (*a*) K. Aoki, M. Satoh, J. Y. Chen and T. Nishiumi, *J. Electroanal. Chem.*, 2006, **595**, 103; (*b*) M. Satoh, K. Aoki and J. Y. Chen, *Langmuir*, 2008, **24**, 4364.
26 S. M. McDonald, J. D. Watkins, Y. Gu, K. Yunus, A. C. Fisher, G. Shul, M. Opallo and F. Marken, *Electrochem. Commun.*, 2007, **9**, 2105.
27 C. Amatore, J.-M. Savéant and D. Tessier, *J. Electroanal. Chem.*, 1983, **147**, 39.
28 W. Miao, J.-P. Choi and A. J. Bard, *J. Am. Chem. Soc.*, 2002, **124**, 14478.
29 A. W. Knight and G. M. Greenway, *Analyst*, 1996, **121**, 101R.
30 (*a*) J. D. Wadhawan, R. G. Evans, C. E. Banks, S. J. Wilkins, R. R. France, N. J. Oldham, A. J. Fairbanks, B. Wood, D. J. Walton, U. Schröder and R. G. Compton, *J. Phys. Chem. B*, 2002, **106**, 9619; (*b*) A. J. Wain, N. S. Lawrence, P. R. Greene, J. D. Wadhawan and R. G. Compton, *Phys. Chem. Chem. Phys.*, 2003, **5**, 1867.
31 *Organic Electrochemistry*, eds. O. Hammerich and H. Lund, Marcel Dekker, New York, 4th edn, 2000.
32 U. Schröder, R. G. Compton, F. Marken, S. D. Bull, S. G. Davies and S. Gilmour, *J. Phys. Chem. B*, 2001, **105**, 1344.
33 C. Amatore, E. Maisonhaute, B. Schöllhorn and J. Wadhawan, *ChemPhysChem*, 2007, **8**, 1321.
34 M. C. Buzzeo, R. G. Evans and R. G. Compton, *ChemPhysChem*, 2004, **5**, 1106.
35 G. K. Rowe and S. E. Creager, *Langmuir*, 1991, **7**, 2307.
36 L. Zhao, Y. Tao and X. Chen, *Acta Chim. Sinica.*, 2006, **64**, 320.
37 Y. Zu and A. J. Bard, *Anal. Chem.*, 2000, **72**, 3223.
38 J.-M. Savéant, *Elements of Molecular and Biomolecular Chemistry*, Wiley-Interscience, New Jersey, 2006.
39 A. R. Despic and J. O'M. Bockris, *J. Chem. Phys.*, 1960, **32**, 389.
40 F. Kanoufi, Y. Zu and A. J. Bard, *J. Phys. Chem. B*, 2001, **105**, 210.
41 *CRC Handbook for Chemistry and Physics*, ed. D. R. Lide, CRC Press, Boca Raton, FL, 76th edn, 1995.
42 J. P. Hawranek and A. S. Muszyński, *J. Mol. Struct.*, 2000, **552**, 205.
43 C. R. Wilke and P. Chang, *Am. Inst. Chem. Eng. J.*, 1955, **1**, 264.
44 D. Pant and H. H. J. Girault, *Phys. Chem. Chem. Phys.*, 2005, **7**, 3457.
45 D. D. Perrin, *Dissociation Constants of Organic Bases in Aqueous Solution*, Butterworths, London, 1965.